

# The negative differential resistance of nitrogen implanted TiO<sub>2</sub>

Chun-Ming Liu

School of Physics, University of Electronic Science and Technology of China, Chengdu 610054, China; [cmliu@uestc.edu.cn](mailto:cmliu@uestc.edu.cn),  
[cmliu028@163.com](mailto:cmliu028@163.com)

## CITATION

Liu CM. The negative differential resistance of nitrogen implanted TiO<sub>2</sub>. *Materials Technology Reports*. 2024; 2(1): 1556.  
<https://doi.org/10.59400/mtr.v2i1.1556>

## ARTICLE INFO

Received: 23 February 2024  
Accepted: 9 April 2024  
Available online: 25 April 2024

## COPYRIGHT



Copyright © 2024 by author(s).  
*Materials Technology Reports* is published by Academic Publishing Pte. Ltd. This work is licensed under the Creative Commons Attribution (CC BY) license.  
<https://creativecommons.org/licenses/by/4.0/>

**Abstract:** The microstructure and negative differential resistance (NDR) effect of nitrogen implanted rutile TiO<sub>2</sub> were investigated by measuring the XPS, Raman spectra and current voltage curves. It was found that the light illumination has large influence on the NDR effect. Under the illumination of 60 mW laser light, a large NDR with a small electric field (1250 V/cm) is obtained. This electric field is about three orders smaller than that reported in literature (1×10<sup>6</sup> V/cm). The electric field induced tunneling is the possible mechanism of electric transport at higher field region. The NDR is thought to be related to the light and nitrogen dopant induced reaction including the destroying of water, the scavenging of electron, and the surface oxidation transform of non-stoichiometric TiO<sub>2-x</sub> to stoichiometric insulating state. The results of this paper are not only useful in understanding the mechanism of NDR, but also useful in providing an effective method in manipulation NDR.

**Keywords:** negative differential resistance; nitrogen implanted TiO<sub>2</sub>; light assistance

## 1. Introduction

More and more attention has been paid to nitrogen doped TiO<sub>2</sub> due to its interesting property and various potential applications including photo catalyst [1–3], diluted magnetic semiconductor [4–6], thermo-electronics [7], electron field emission [8] and electrical transport property [9,10]. It is found that oxygen vacancy can be favorably generated in nitrogen doped TiO<sub>2</sub> since the formation energy of oxygen vacancy in TiO<sub>2</sub> is largely decreased by nitrogen doping [1]. TiO<sub>2</sub> is changed from insulator to semiconductor since the electrical resistivity of TiO<sub>2</sub> was reduced by the formation of oxygen defects [7]. The band gap of TiO<sub>2</sub> can be effectively decreased. The photo catalyst activity under visible light can be greatly enhanced [1–3]. Magneli phase of Ti<sub>n</sub>(O, N)<sub>2n-1</sub> can also be obtained [7]. Furthermore, it was found that the oxygen vacancy of nitrogen doped TiO<sub>2</sub> has better stability than that of pure TiO<sub>2</sub> [8].

It is well known that the generation and redistribution of oxygen vacancies are closely related to many interesting phenomena such as the NDR and the resistance switching (RS) of TiO<sub>2</sub> [11–15]. For example, the generated oxygen vacancies can migrate under bias voltage and then form conductive filaments [14]. Once two metal electrodes are connected by conductive filaments, materials are changed from high resistance state to low resistance state because current can pass through these filaments. On the other hand, due to the Joule heat or the ionic migration, filaments rupture and materials are changed into high resistance state. However, there are few reports on NDR and RS of nitrogen doped TiO<sub>2</sub>.

The NDR and RS effect of TiO<sub>2</sub> have been studied intentionally as there are a lot of potential applications such as the resonant tunneling transistors, oscillators, multipliers, and resistive random-access memory [11–16]. NDR and RS of TiO<sub>2</sub> were thought to be related to the oxygen vacancies, phase changing and electrical

chemical reaction. For example, Kim et al. [11] indicated that NDR is the result of local surface oxidation under bias voltage. The electrical current maximum state is obtained as the oxygen vacancies are formed and subsequently ordered and ultimately led phase change from a nonconductive fully-oxidized phase to a conductive oxygen-deficient Magnéli phase [11]. The electrical current minimum state is obtained when the non-stoichiometric  $\text{TiO}_2$  transforms to the stoichiometric insulating state. Zhao et al. [13] assigned the NDR to the damage of hydrogen-bonds among water molecules to break the continuous water layer. Wang et al. [12] assigned the NDR of  $\text{Pt/BiFeO}_3/\text{TiO}_2/\text{BiFeO}_3/\text{Pt}$  to the polarization field in the two  $\text{BiFeO}_3$  layers which causing the movement of electrons to be bound. Kamaladasa et al [16] found that the bias voltage induced reversible bipolar RS in  $\text{TiO}_2$  is accompanied with the reversible formation and dissociation of shear faults. The shear faults are induced by the increasing of oxygen vacancy concentration to some extent [16].

## 2. Experiments

Experimentally, the single crystal  $\text{TiO}_2$  substrates were available from Hefei Kejing Materials Technology Co.Ltd. The nitrogen implantation was performed at the energy of 60 keV in a vacuum chamber of  $2 \times 10^{-3}$  Pa, with the nominal dose of  $1 \times 10^{18}$  ions  $\text{cm}^{-2}$ . The substrate was kept at room temperature by the circulation of cooling water during ion implantation. The samples' stoichiometry was measured by a KRATOS X SAM 800 x-ray photoelectron spectroscopy (XPS). Raman spectra were obtained by a HORIBA LABRAM HR laser Raman spectrometer. The current voltage curve was measured using two terminal methods. The distance between the two electrodes is about 2 mm. The sample size for I-V measurement is about  $4 \times 5 \times 0.5$  mm<sup>3</sup>. The light illumination is using a laser with the wavelength of 405 nm. The laser beam diameter is about 2.5 mm.

## 3. Results and discussions

In a previous paper [4], the microstructure, light absorption, magnetism and electrical transport property of nitrogen implanted  $\text{TiO}_2$  single crystal were investigated. It was found that the nitrogen implanted  $\text{TiO}_2$  is with a single rutile crystal structure. The absorption in the visible light region is greatly enhanced with nitrogen implantation. Room-temperature ferromagnetism is obtained in the sample with an implanted dose of about  $1 \times 10^{18}$  ions/ $\text{cm}^2$ . The sample changes from insulating to semiconductor when nitrogen doping increasing to  $1 \times 10^{18}$  ions/ $\text{cm}^2$ . The incorporation of nitrogen is confirmed by XPS measurements.

**Figure 1** shows the full-survey and high resolution XPS of the sample with an implantation dose of about  $1 \times 10^{18}$  ions/ $\text{cm}^2$ . Obviously seen in the full-survey spectrum, only four elements, Ti, N, O, and C, are found in this sample. The signal from carbon is mainly introduced by the surface contamination during the XPS measurement. There are no other elements being detected by XPS. The high-resolution N1s spectrum has a broad spectrum ranged from 395eV to 404eV, with the maximum located at about 401 eV. This behavior is similar as that reported in literature [3,17]. The high-resolution N1s spectrum can be fitted by two peaks

located at 399.4 and 402.0 eV, respectively. The peak near 399.4 eV was ascribed to interstitial nitrogen doping with structure of Ti–O–N [10]. The peak near 402 eV was ascribed to titanium oxynitrides [9] or to substantial nitrogen doping with structure of O–Ti–N [3]. It should be kept in mind that the nitrogen state in the doped TiO<sub>2</sub> varies from case to case. For example, peaks at 396–397 eV were attributed to substitutional nitrogen [9]. Peaks at higher binding energies (~400 eV) were ascribed to a generic interstitial site [1]. In the other hand, the signal at 401.3 eV was attributed substitutional nitrogen [3]. The high resolution Ti 2p<sub>3/2</sub> spectrum can be fitted by two peaks located at 458.2 and 458.8 eV. The peak at 458.8 eV was ascribed to stoichiometry TiO<sub>2</sub> crystals. The peak at 458.2 eV was assigned to nitrogen doped TiO<sub>2</sub> structure [8]. There is a 0.6 eV shift to lower binding energy for nitrogen doped TiO<sub>2</sub>, which indicates the increasing in electron density around Ti atoms in the nitrogen-doped TiO<sub>2</sub> [8]. The formation of oxygen vacancies induced by nitrogen doping was thought to be responsible for the electron density increasing by reducing the valence state of Ti<sup>4+</sup> to lower states Ti<sup>3+</sup> [8]. The high resolution O1s spectrum can be fitted by two peaks located at about 530.8 and 529.9 eV, respectively. The peak near 530.8 eV was assigned to TiO<sub>2</sub>. The peak near 529.9 eV was ascribed to nitrogen doped TiO<sub>2</sub> structure [3].

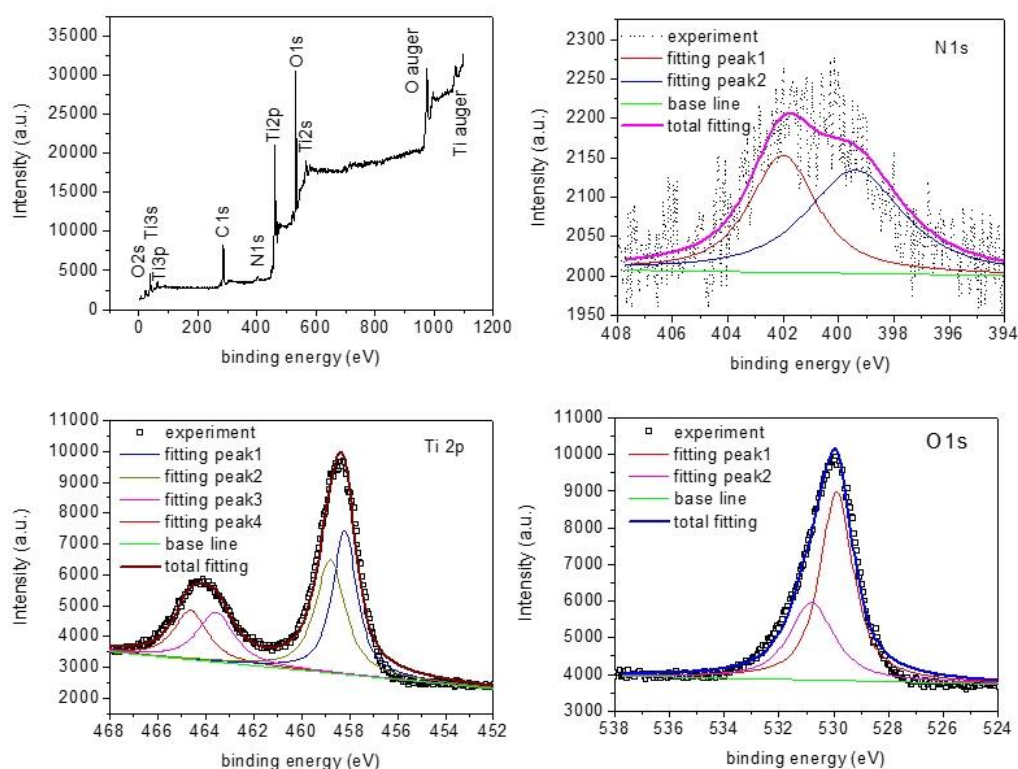


**Figure 1.** The full-survey and high resolution XPS of the nitrogen implanted TiO<sub>2</sub> sample.

**Figure 2** shows the Raman spectra of nitrogen implanted TiO<sub>2</sub> sample. There are peaks located at about 141, 237, 445, and 611 cm<sup>-1</sup> in the Raman spectra, which can be assigned to the B<sub>1g</sub> (141 cm<sup>-1</sup>), two phonon processes E<sub>g</sub> (237, 448 cm<sup>-1</sup>), and A<sub>1g</sub> (611 cm<sup>-1</sup>) Raman active modes of the rutile phase TiO<sub>2</sub> [10]. There are no fundamental Raman active modes from anatase phase titanium dioxide including A<sub>1g</sub> (519 cm<sup>-1</sup>), B<sub>1g</sub> (399 cm<sup>-1</sup>) and E<sub>g</sub> (197 and 639 cm<sup>-1</sup>) [18], indicating that the

sample is of pure rutile structure.

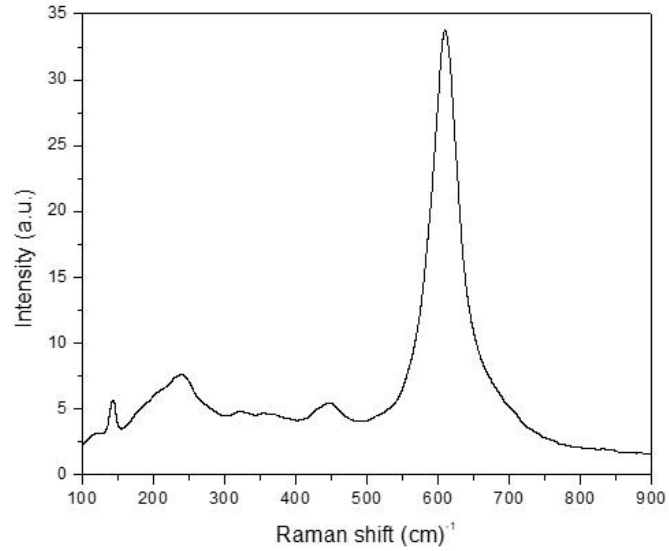
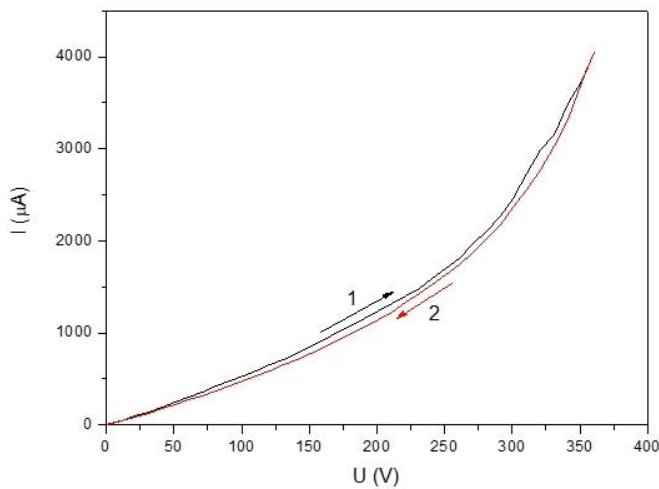
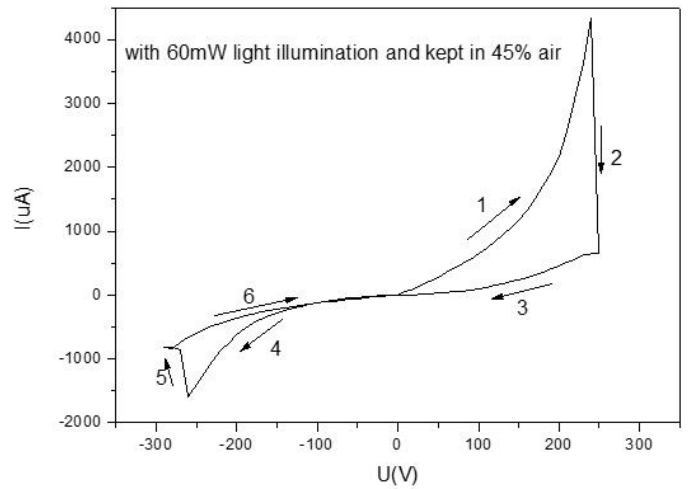


**Figure 2.** Raman spectra of nitrogen implanted  $\text{TiO}_2$  sample.

The current–voltage (I–V) curve of nitrogen implanted  $\text{TiO}_2$  sample is shown in **Figure 3a,b**. As seen in **Figure 3a**, without light illumination, there is no NDR in the bias voltage region from 0 to 350 V. The current increases non-linearly with voltage increasing. There is little hysteresis between the I–V curves measured with voltage varying from 0 to 350 and then back to 0 V. This behavior indicates that there are little RS effect and NDR without light assistance. The reason should be due to that the bias voltage is not large enough [14]. When the bias voltage is small, it may only generate electronic current and little influence on the chemical or physical state of the materials, and in this situation, the I–V curves are non-hysteretic and closed. When the bias voltage is high enough, the ionic movements and/or the redox reactions are likely to initiate to alter the chemical or physical state of the materials, and in this case, the I–V curves are expected to become hysteretic and open [14]. Since NDR in  $\text{TiO}_2$  usually appears with an electric field of about  $1 \times 10^6$  V/cm [19], the bias voltage should be about  $2 \times 10^5$  V to induce NDR for our sample.



**(a)**



**(b)**

**Figure 3.** The current–voltage (I-V) curve of nitrogen implanted TiO<sub>2</sub> sample. (a) without light; (b) with light illumination. The number in (a) and (b) is the measuring sequence.

Different from **Figure 3a,b** shows that there is a large hysteresis in the I-V curve when the sample is illuminated with a 60 mW laser. The current increases from 0 to 4326  $\mu\text{A}$  when the bias voltage increases from 0 to 240 V. The current then decreases from 4326  $\mu\text{A}$  to 661  $\mu\text{A}$  when the bias voltage further increases from 240 to 250 V. The ratio of current peak to current valley is about 7. The I-V curve in the positive bias region is different from that in the negative bias region. So, it is not symmetric. In the negative bias region, the current increases to  $-1590 \mu\text{A}$  when the bias voltage is ramped up to  $-260 \text{ V}$ . the current then decreases to  $-854 \mu\text{A}$  as the voltage is further increased to  $-270 \text{ V}$ . The ratio of current peak to current valley is about 2. Therefore, this NDR is not repeatable and reduces quickly. It is evidently seen that light illumination plays an important role in NDR. The large number of photo-generated charge carriers and the enhanced polarization of BiFeO<sub>3</sub> were thought to be responsible for the NDR and RS [12]. The light-enhanced NDR was also reported in MoS<sub>2</sub> quantum dots sample [20]. The electric field to induce NDR in our sample with the assistance of light is about  $1.25 \times 10^3 \text{ V/cm}$ . This is about three orders smaller than that reported [19]. There is a large reduction in electric field with the assistance of light. This behavior was not reported in the previous literatures [20].

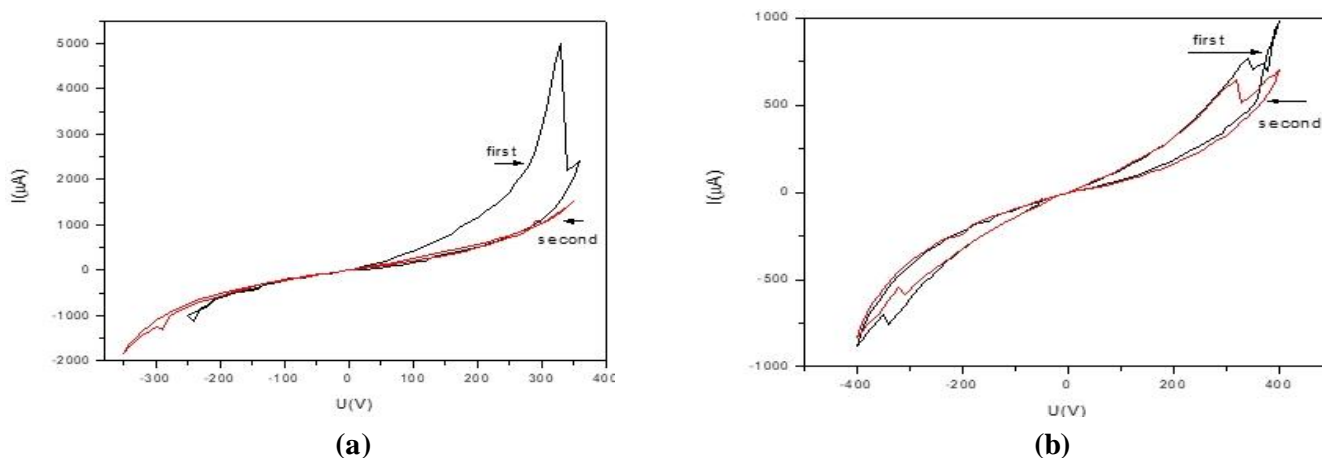


**Figure 4.** The NDR of sample kept at different humidity environment. (a) with 45% RH; (b) with 24% RH. The black and red curves are the first and second cycle measured I-V curves, respectively.

**Figure 4** shows the NDR of sample kept at different humidity environment, respectively. As seen in **Figure 4**, the NDR in our sample is sensitive to the environment moisture. The NDR is largely recovered when the sample was kept in wet air with a humidity of 45% RH for about 5 days (**Figure 4a**). The ratio of current peak to the current valley is about 2.3. There is large hysteresis in the I-V curve obtained at the first bias voltage changing cycle ( $0 \rightarrow 350 \rightarrow 0 \rightarrow -350 \rightarrow 0 \text{ V}$ ). The hysteresis in the I-V curve becomes very weak in the second voltage changing cycle. In the other hand, the NDR is a little recovered when the sample was kept in dry air with a humidity of about 24% RH for 5 days. The current peak to valley ration is only about 1.3. The I-V curve in **Figure 4b** is almost similar for the two bias voltage changing cycles. The I-V curve in **Figure 4b** is almost similar for the positive bias

region and the negative bias region. In one voltage changing cycle, the bias voltage varies from  $0 \rightarrow 400 \rightarrow 0 \rightarrow -400 \rightarrow 0$  V. The difference in I-V curve measured in different humidity means that atmosphere plays important role in NDR of nitrogen implanted  $\text{TiO}_2$ . This behavior is similar as that reported in literature [13].

**Figure 5** shows the current (I) as a function of voltage (U) in the higher field region. As seen in **Figure 5**, in the higher field region, the logarithmic of I/U is proportional to the  $1/U$ , i.e.,  $\ln(I/U) \propto 1/U$ . This behavior is the character of metal-insulator granular films at high electric field region where the current is dominated by field induced tunneling [21]. In the case of our sample, the nonconductive fully-oxidized phase of titanium oxides (TO) plays the role of insulator. The water and conductive oxygen-deficient phase of titanium oxides ( $\text{TO}_x$ ) can play the role of metal grains. It was thought that large amount of hydrogen ions can emerge from the ionization of water molecules to create electric current [13]. These conducting grains are randomly distributed and separated by insulator TO barrier. The current carriers transport by tunneling through the insulating barrier separating the conducting grains. This tunneling mechanism is hold in all cases (with light illumination or without light illumination. Before NDR or after NDR). The changing from  $\text{TO}_x$  to TO would increase the thickness of tunneling barrier and further reduce the tunneling current. On the contrary, the changing from TO to  $\text{TO}_x$  would decrease the thickness of tunneling barrier and further increase the tunneling current. The desorption (adsorption) of water would also increase (decrease) the tunneling distance and further lead the reduction (enhancement) of tunneling current.

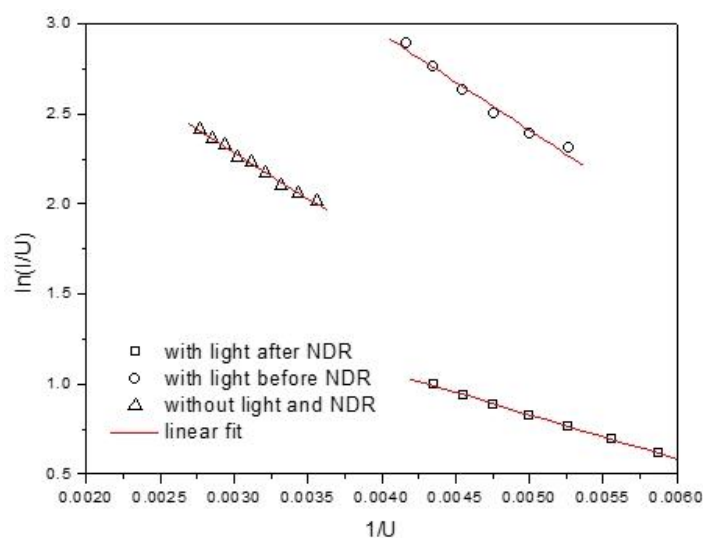


**Figure 5.** The dependence of  $\ln(I/U)$  on  $1/U$  in the higher field region.

Based on the above experiments, the mechanism of NDR of nitrogen implanted  $\text{TiO}_2$  should be partly related to the environmental moisture. Water molecular would be adsorbed in the nitrogen implanted  $\text{TiO}_2$  sample [13]. With light illumination, a lot of electrons and holes are generated by photo. Some of the photo generated electrons and holes will migrate to the surface of sample, while others are recombined. Under the influence of electrical field, the generated electrons and holes are further separated by large enough electric field and transport so that the current increases rapidly under a certain electrical field. Large Joule heat will be generated in the case

of large current. The water molecular will be destroyed by Joule heat and the current is decreased [13]. Once the water is destroyed, there need a time period for water adsorption until the water is recovered again. Therefore, the I-V curve is not symmetrical and not repeatable in wet environment. In addition, the light illumination not only generates electron and hole pairs but also the photo catalyst effect. The photo catalyst can destroy water by changing water molecular into hydrogen and oxygen gas.

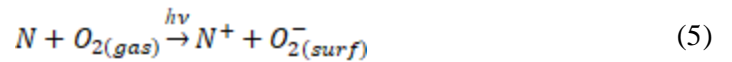
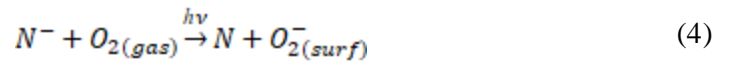
Besides the effect of moisture, the oxygen molecular and oxygen vacancy should also be considered. As shown in equation (1), the oxidation of lattice oxygen ( $O_o^x$ ) and the formation of oxygen vacancies ( $V_o$ ) in the vicinity are possible [14,22]. This reaction leaves behind two electrons and oxygen vacancy. The generated oxygen vacancies can migrate to form the conductive filaments. This further leads the increasing of electric current. In the reverse reactions, electrons and oxygen vacancy can be reduced and leading the reduction of current [22]. In the other hand, the electron can be scavenged by the adsorbed  $O_2$  and produce adsorbed  $O_2^-$  [14]. The photo catalyst can also scavenge the current carriers by producing radicals such as  $H_2O\cdot$ ,  $OH\cdot$ , and  $O_2\cdot$  [17].



With light illumination and nitrogen doping, it is advantage not only for the exciting of electron and hole, but also for the scavenging of electron [1]. Irradiation under vacuum with light selectively promotes electrons from nitrogen atom impurities to the conduction band according to the following process (2) and (3) [1].



On the other hand, the presence of oxygen in the gas phase modifies the situation as a fraction of photo excited electrons is scavenged by  $O_2$  producing adsorbed  $O_2^-$  (process (4) and (5)) [1].



The nitrogen atom impurities exist either as charged centers ( $N^-$ ) or as neutral centers (N) in  $TiO_2$  [1]. Under the light irradiation with an energy of  $h\nu$ , electrons are promoted from the localized N-impurity states ( $N^-$  and N) to the electron scavengers like  $O_2$  in environment ( $O_{2(gas)}$ ). Then the  $O_2$  in environment becomes negative charged and adsorbed on the surface ( $O_{2(surf)}^-$ ). The electric current will be reduced by these electron scavengers. Furthermore, the surface adsorbed  $O_2^-$  will heal the defect sites such as oxygen vacancies and  $Ti^{3+}$  interstitials [23]. This will lead non-stoichiometric  $TiO_{2-x}$  transform to the stoichiometric insulating state, resulting in the NDR effect [11]. The surface oxidation can be reversed by local reduction [11]. The NDR due to surface oxidation should be reversible and repeatable.

## 4. Conclusion

In summary, with the assistance of visible light illumination, a negative differential resistance (NDR) with small electric field ( $\sim 1250$  V/cm) and a large peak to valley ratio ( $\sim 7$ ) is obtained in nitrogen implanted TiO<sub>2</sub> single crystal. The NDR is related to the environment moisture. In higher humidity environment, the ratio of current peak to current valley is higher. However, the NDR in higher humidity is not reversible because the diffusion of water in sample is not fast enough. The possible mechanism of transport and NDR is discussed. The NDR should be related to the nitrogen dopants and the visible light induced reaction such as the destroy of the adsorption water, the scavenging of electron, and the surface oxidation transform of non-stoichiometric TiO<sub>2-x</sub> to stoichiometric insulating state.

**Funding:** This study was supported financially by National Natural Science Foundation of China (Grant No 10904008), the Agricultural Public Welfare Project of Sichuan Province of China (grant no.2015NZ0098), and the Fundamental Research Funds for The Central Universities (grant no.ZYGX2016J062).

**Conflict of interest:** The author declares no conflict of interest.

## References

- Di Valentin C, Finazzi E, Pacchioni G, et al. N-doped TiO<sub>2</sub>: Theory and experiment. *Chemical Physics*. 2007; 339(1-3): 44-56. doi: 10.1016/j.chemphys.2007.07.020
- Wang H, Lewis JP. Second-generation photocatalytic materials: anion-doped TiO<sub>2</sub>. *Journal of Physics: Condensed Matter*. 2005; 18(2): 421-434. doi: 10.1088/0953-8984/18/2/006
- Chen X, Burda C. Photoelectron Spectroscopic Investigation of Nitrogen-Doped Titania Nanoparticles. *The Journal of Physical Chemistry B*. 2004; 108(40): 15446-15449. doi: 10.1021/jp0469160
- Liu CM, Xiang X, Zhang Y, et al. Magnetism of a Nitrogen-Implanted TiO<sub>2</sub> Single Crystal. *Chinese Physics Letters*. 2011; 28(12): 127201. doi: 10.1088/0256-307x/28/12/127201
- Tao JG, Guan LX, Pan JS, et al. Density functional study on ferromagnetism in nitrogen-doped anatase TiO<sub>2</sub>. *Applied Physics Letters*. 2009; 95(6). doi: 10.1063/1.3204463
- Bao NN, Fan HM, Ding J, et al. Room temperature ferromagnetism in N-doped rutile TiO<sub>2</sub> films. *Journal of Applied Physics*. 2011; 109(7). doi: 10.1063/1.3535427
- Mikami M, Ozaki K. Thermoelectric properties of nitrogen-doped TiO<sub>2-x</sub> compounds. *Journal of Physics: Conference Series*. 2012; 379: 012006. doi: 10.1088/1742-6596/379/1/012006
- Liu G, Li F, Wang DW, et al. Electron field emission of a nitrogen-doped TiO<sub>2</sub> nanotube array. *Nanotechnology*. 2007; 19(2): 025606. doi: 10.1088/0957-4484/19/02/025606
- Yu YP, Liu W, Wu SX, et al. Impact of Nitrogen Doping on Electrical Conduction in Anatase TiO<sub>2</sub> Thin Films. *The Journal of Physical Chemistry C*. 2012; 116(37): 19625-19629. doi: 10.1021/jp300024n
- Yen Y, Ou S, Lin K. One-Pot Synthesis of Nitrogen-doped TiO<sub>2</sub> Nanowires with Enhanced Photocurrent Generation. *Journal of the Chinese Chemical Society*. 2017; 64(12): 1392-1398. doi: 10.1002/jccs.201700226
- Kim Y, Jang JH, Park SJ, et al. Local probing of electrochemically induced negative differential resistance in TiO<sub>2</sub> memristive materials. *Nanotechnology*. 2013; 24(8): 085702. doi: 10.1088/0957-4484/24/8/085702
- Wang X, Wang Y, Feng M, et al. Light-induced negative differential resistance effect in a resistive switching memory device. *Current Applied Physics*. 2020; 20(3): 371-378. doi: 10.1016/j.cap.2019.12.008
- Zhao X, Chen X, Ding X, et al. Humidity Sensing Properties and Negative Differential Resistance Effects of TiO<sub>2</sub> Nanowires. *IEEE Sensors Journal*. 2021; 21(17): 18477-18482. doi: 10.1109/jsen.2021.3091536
- Lu W, Wong LM, Wang S, et al. Effects of oxygen and moisture on the I-V characteristics of TiO<sub>2</sub> thin films. *Journal of Materiomics*. 2018; 4(3): 228-237. doi: 10.1016/j.jmat.2018.01.005



15. Liu S, Liu B, Wang T, et al. High anisotropic magnetoresistance, perfect spin-filtering effect, and negative differential resistance effect of Cr-doped anatase phase TiO<sub>2</sub>. *Physica Scripta*. 2022; 98(1): 015827. doi: 10.1088/1402-4896/aca74
16. Kamaladasa RJ, Sharma AA, Lai YT, et al. In Situ TEM Imaging of Defect Dynamics under Electrical Bias in Resistive Switching Rutile-TiO<sub>2</sub>. *Microscopy and Microanalysis*. 2014; 21(1): 140-153. doi: 10.1017/s1431927614013555
17. Chen X, Lou YB., Samia ACS, et al. Formation of Oxynitride as the Photocatalytic Enhancing Site in Nitrogen-Doped Titania Nanocatalysts: Comparison to a Commercial Nanopowder. *Advanced Functional Materials*. 2005; 15(1): 41 -49. doi: 10.1002/adfm.200400184
18. Mahalingam S, Edirisinghe MJ. Novel preparation of nitrogen-doped titanium dioxide films. *Journal of Physics D: Applied Physics*. 2008; 41(21): 215406. doi: 10.1088/0022-3727/41/21/215406
19. Chopra KL. Avalanche-Induced Negative Resistance in Thin Oxide Films. *Journal of Applied Physics*. 1965; 36(1): 184-187. doi: 10.1063/1.1713870
20. Sharma S, Chen Y, Santiago SRMS, et al. Light-Enhanced Negative Differential Resistance and Multi-Level Resistive Switching in Glutamine-Functionalized MoS<sub>2</sub> Quantum Dots for Resistive Random-Access Memory Devices. *Advanced Materials Interfaces*. 2022; 10(2). doi: 10.1002/admi.202201537
21. Sheng P, Abeles B, Arie Y. Hopping Conductivity in Granular Metals. *Physical Review Letters*. 1973; 31(1): 44 -47. doi: 10.1103/physrevlett.31.44
22. Cooper D, Baeumer C, Bernier N, et al. Anomalous Resistance Hysteresis in Oxide ReRAM: Oxygen Evolution and Reincorporation Revealed by In Situ TEM. *Advanced Materials*. 2017; 29(23). doi: 10.1002/adma.201700212
23. Stevanovic A, Büttner M, Zhang Z, et al. Photoluminescence of TiO<sub>2</sub>: Effect of UV Light and Adsorbed Molecules on Surface Band Structure. *Journal of the American Chemical Society*. 2011; 134(1): 324-332. doi: 10.1021/ja2072737